Scientific Research Publishing

Open Journal of Applied Sciences, 2023, 13, 1119-1144
https://www.scirp.org/journal/ojapps
ISSN Online: 2165-3925
ISSN Print: 2165-3917

Adsorption of Natural Surfactant on Sandstone in Enhanced Oil Recovery: Isotherms and Kinetics Studies

Monday Obekpa Michael

Department of Petroleum Engineering, Khazar University, Baku, Azerbaijan
Email: mondaymichael.12@gmail.com

How to cite this paper: Michael, M.O. (2023) Adsorption of Natural Surfactant on Sandstone in Enhanced Oil Recovery: Isotherms and Kinetics Studies. *Open Journal of Applied Sciences*, **13**, 1119-1144.
https://doi.org/10.4236/ojapps.2023.137090

Received: June 5, 2023
Accepted: July 24, 2023
Published: July 27, 2023

Abstract

In chemical enhanced oil recovery, surfactants are injected into the reservoir with the intention to lower interfacial tension (IFT) between the water and oil phases, and thereby bring about efficient displacement of oil. However, the adsorption of the surfactants to reservoir rock surfaces leads to the loss and reduction in concentration of the surfactants, which in turn reduces the overall efficiency of the oil recovery process, with attendant financial losses. In this work, the adsorption of Quillaja Saponaria (QS), a novel, natural, non-ionic surfactant, on crushed sandstone reservoir rock is investigated. X-ray diffraction (XRD) study of clean sandstone particles has been undertaken to determine the main components present in the sand particles. The conductivity method was used to measure CMC and the surfactant concentrations in aqueous solutions. Batch adsorption experiments were used to determine the amount of QS adsorbed on rock surface. Equilibrium conditions were reached after almost 5 days. From the results of the study, the Langmuir isotherm model is more suited for predicting the adsorption behaviour of QS on sandstone. The kinetic adsorption of QS obeys the pseudo-second order model. This study is particularly relevant in surfactant selection for chemical EOR processes.

Keywords

Enhanced Oil Recovery, Critical Micelle Concentration, Interfacial Tension, Adsorption Kinetics, Surfactant, Saponin

1. Introduction

About 60% of all worldwide petroleum reservoirs are sandstone; aside from the Middle East, the proportion is even much higher in other parts of the globe.

These sandstone reservoirs are mostly composed of stable minerals (such as feldspar, quartz, rock fragments), accessory minerals, and pores saturated with fluids such as oil, gas, and groundwater [1] [2]. The average recovery factor (RF), the ratio of recoverable oil to the volume of oil originally in place (OOIP), for all reservoir types is about 35%, and sandstone reservoirs tend to have better RFs than carbonates [3]. One chemical EOR method used to increase the RF is surfactant flooding. Surfactant flooding has been used to increase the RF to about 50% of OOIP [4]-[13]. The use of surfactants to enhance oil recovery comes in various forms, including surfactant-polymer (SP) flooding, alkali-surfactant-polymer (ASP) flooding, surfactant-micellar injection, as well as surfactant huff-n-puff processes [14] [15] [16].

Surfactants or surface-active agents are chemical compounds characterised by the possession of medium-to-long-chain molecular structures with both hydrophilic ("likes" water) and hydrophobic ("dislikes" water) moieties that tend to be distributed at the interface between the liquid phases, with varying degree of polarity (*i.e.* oil/water) [17] [18]. The hydrophilic portion is usually polar or ionic, while the hydrophobic portion is generally in the form of long-chain non-polar hydrocarbons. Surfactants are characterised by properties such as critical micelle concentration (CMC), hydrophilic-lipophilic balance (HLB), chemical structure and charge, as well as properties from their origin or source material [19] [20]. The surfactants exist as monomers or single molecules at low concentrations in aqueous solutions; beyond the CMC, the surfactant molecules assemble together to form aggregates or micelles The adsorption of surfactant particles follows different patterns, and their arrangement in the adsorbed phase is typically different from that in the bulk fluid phase. Irrespective of the phase that the particles are adsorbed onto, the surfactant monomers in the aqueous solution will be in equilibrium with both micelles and adsorbate [15]. **Figure 1** shows the relationship between a surfactant property (in this case, surface tension) and surfactant concentration, with the CMC being the point where surfactant property stabilizes.

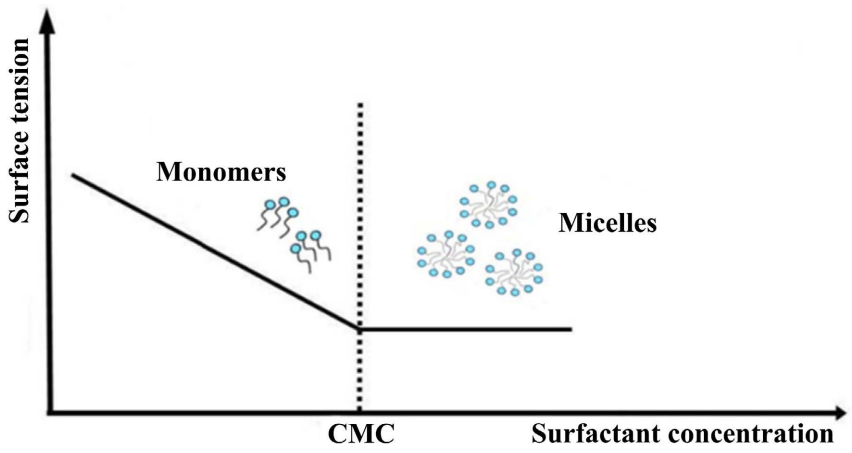

Figure 1. Critical micelle concentration of a surfactant [21].

Typically, chemical EOR processes are affected by a number of factors, such as interaction between surfactants and formation fluids, heterogeneity of porous medium, surfactant adsorption onto the solid rock surface, and the coalescence of oil droplets [22]. Of particular importance is the loss of surfactants through sorption and retention in the reservoir rock, which has implications on the efficiency and economy of the overall process.

Surfactants are used for the stimulation of hydrocarbon reservoirs and enhanced recovery processes, which often leads to higher recovery of oil from the reservoirs. It is therefore economically imperative to reduce the amount of surfactant adsorption or loss to rock surface. The adsorption of surfactants to solid surfaces can occur through a number of mechanisms, namely: ion exchange, ion pairing, hydrophobic bonding, π electron polarisation and dispersion forces [23] [24] [25] [26]. Despite the complex nature of adsorption (because it combines mass transfer and reaction kinetics unit operations), researchers have been able to identify some factors that affect surfactant adsorption; they include ionic strength, pH, temperature, adsorbent amount, and electrolyte concentration [27] [28] [29] [30] [31].

The adsorption of natural surfactants on reservoir rock surfaces (carbonate and sandstone) is an essential aspect of chemical EOR and soil remediation, hence the reason why several studies have been carried out on them and reported in literature; some are provided in Refs. [22] [23] [32] [33] [34]. Researchers have been able to show that the main driving forces behind surfactant adsorption are the surfactant type, physical (lithology) and chemical properties of reservoir rocks, as well as the chemistry of the bulk solution [33] [35]. Scamehorn (1980), in his dissertation, investigated the adsorption of a dilute solution of sodium alkyl benzene sulfonate on clay minerals, and concluded that the Langmuir isotherm matched his data set, and therefore was the most appropriate [36]. Muherei and Junin (2009) performed a comparative study of the adsorption of Polyethylene glycol tert-octylphenyl ether-Triton X100 (TX100), a non-ionic surfactant, and Sodium Dodecylsulfate (SDS), an anionic surfactant, on shale and sandstone. It was observed that while Triton X100 was adsorbed to both adsorbents, SDS was not detected on either of the adsorbent samples. Additionally, the adsorption data for lower than CMC concentrations successfully fit both the Freundlich and Langmuir isotherms, with the Freundlich model showing a much better correlation [37]. Azam *et al.* (2013) studied the static adsorption of a novel in-house synthesised surfactant on Berea sandstone and discovered that only a very minimal amount of surfactant was adsorbed (0.96 mg/g) at higher pH, higher temperature and lower salt concentration [38]. Ahmadi and Shadizadeh (2016) investigated the adsorption equilibrium of Zyziphus spina-christi, a natural surfactant onto a sandstone rock sample. In their work, they analyzed the results with 2 very common adsorption isotherms and based on the coefficient of determination value (R^2) concluded that the Freundlich model was a better fit for the adsorption equilibrium of Zyziphus spina-christi [39]. Zendehboudi *et al.* (2013) also worked on the adsorption of Zyziphus spina-christi

(ZSC) but on carbonate rocks, and determined that the adsorption behaviour was well predicted by the Freundlich isotherm. In addition, they showed that ZSC was able to increase the recovery factor from a carbonate reservoir from 47% to 77% [22].

In 2011, Stanimirova *et al.* [40] worked on Quillaja Saponaria (QS) with the intention of determining its rheological surface properties. They concluded that QS exhibits properties consistent with those of any non-ionic surfactants and that the Volmer and Langmuir adsorption isotherms best describe the adsorption behaviour of QS for non-localised and localised adsorption of molecules, respectively [40]. In his MSc research work, Beach, B.A. (2016) demonstrated that saponins derived from the Quillaja soapbark tree could be used as an alternative surfactant in the remediation of soil contaminated with non-aqueous phase liquid (NAPL) [34]. The results of the test showed that Quillaja saponria had a much lower CMC value (0.006 wt%) than its synthetic counterpart, Biosolve, and it significantly enhanced the solubilisation of polycyclic aromatic hydrocarbons (PAHs) [34].

In this study, static adsorption of Quillaja Saponaria (QS), a natural non-ionic surfactant, by crushed sandstone rocks is investigated at 298K and in different aqueous concentrations for the purpose of implementation in chemical EOR. The CMC of QS was determined using the conductivity method. Furthermore, 4 well known adsorption isotherms were investigated with a view to determining the adsorption parameters for QS; the adsorption isotherm models examined include: Freundlich, Langmuir, Temkin, and Linear.

2. Material and Experimental Investigation

2.1. Surfactant

Quillaja Saponaria (QS), also known as soap bark tree or Quillay, is an evergreen tree in the family of Quillajaceae that is indigenous to warm, temperate central Chile, Peru and Bolivia [41]. The saponin content varies depending on a number of factors, such as age of plant, component of plant used for extraction of saponin, environmental factors, and genetic origin of plant [42]. Saponins are natural surface–active substances synthesized from different plants species, lower marine animals, and some bacteria [43] [44]. Saponin molecules contain a hydrophobic part, composed of a triterpenoid or steroid backbone, and a hydrophilic part, which consists of several saccharide residues, attached to the hydrophobic scaffold via glycoside bonds [40]. The combination of a non-polar sapogenin and water-soluble side chain in saponins confers on them emulsifying and forming abilities which are highly sought after in many industrial applications such as beer, food, and detergent making processes.

The Quillaja Saponaria (QS) sample used in this study was sourced from Desert King, Chile S.A. The properties of QS used in this study (as provided in the material safety data sheet, MSDS) are presented in **Table 1**. **Figure 2** is a schematic of the general molecular formula of QS.

Table 1. Properties of quillaja saponaria (QS).

Test	Specification	Results
Appearance	Light brown free-flowing powder	Light brown free-flowing powder
Absorbance	≤1.500 (10% w/w, at 520 nm)	0.553
pH	4.1 ± 0.2 (20%w/w solution)	4.1
Moisture (%)	<7.0	1.0
Saponin (%)	>20 (UPLC C18 analytical method)	23.4
Tannins (%)	-	3.0
Preservatives	None	None
Total Plate Count (cfu/g)	<100	<10
Mold (cfu/g)	<100	<10
Yeast (cfu/g)	<100	<10

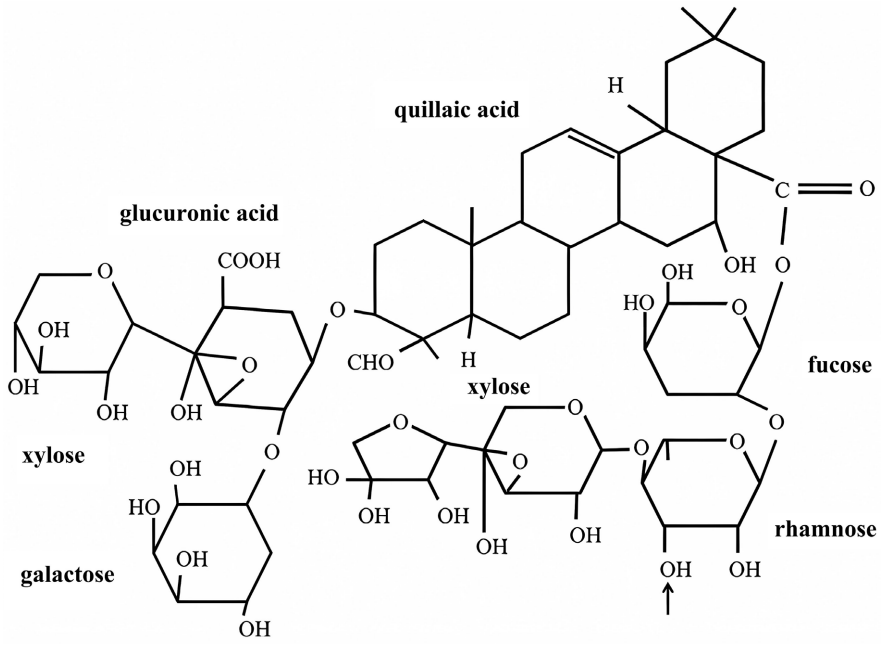

Figure 2. General molecular structure of Quillaja Saponins [45].

2.2. Adsorbent

Sandstone samples used for this study were obtained from the Absheron field in the Azerbaijani sector of the Caspian Sea. The chemical and mineralogical compositions of the rock sample are provided in **Figure 3** and **Figure 4** respectively. The cores were crushed with mortar and pestle and ground into a powder. The crushed rock samples were then sieved with a mechanical sieve to obtain particles with an average size of 354 μm. The crushed samples were air-dried for 24 hours and then oven-dried at 105˚C for another 48 hours.

In addition, the mineral composition of the sandstone powder determined by X-Ray Diffraction (XRD) is shown in **Figure 5**. From the analysis, the vast majority

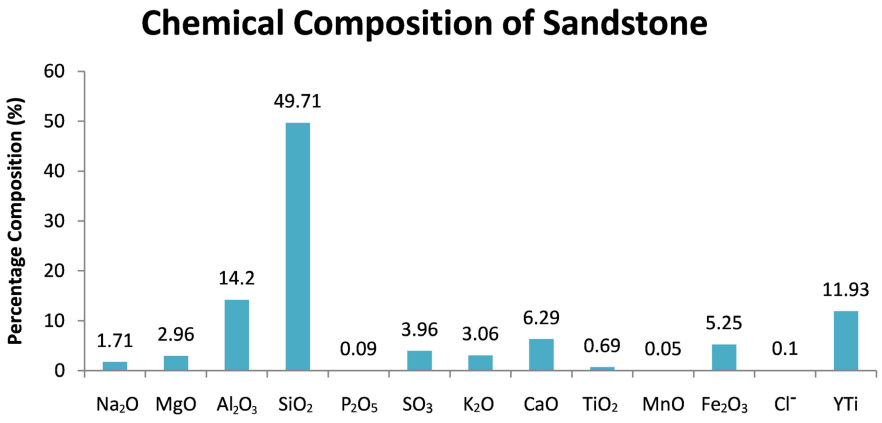

Figure 3. Chemical composition of sandstone (YTi = the quantity of evaporated components at 950˚C).

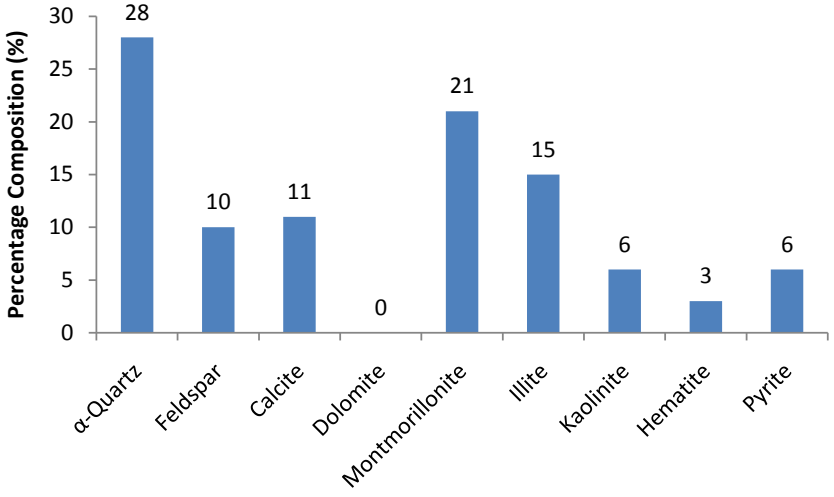

Figure 4. Mineral composition of sandstone.

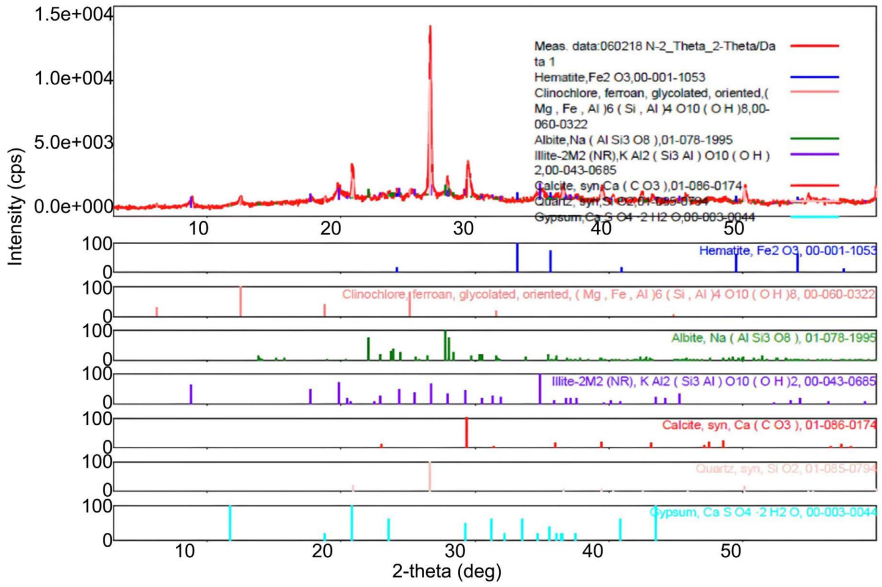

Figure 5. X-ray diffraction (XRD) result of the crushed sandstone used in test.

of the chemical and mineral content of the sandstone rock used is Quartz (28%), closely followed by Montmorillonite (21%).

3. Preparation of Surfactant Solution

A stock solution of QS with different concentrations was prepared using a known quantity of the QS powder diluted in 1000 mL of deionised water in a volumetric flask. Deionised water was used in order to prevent the interaction of dissolved particles with the QS powder. A magnetic stirrer was used to ensure a homogenous mixture. Afterwards, the stock solution was diluted using dilution rule to obtain concentrations of QS ranging from 100 mg/L to 1000 mg/L.

3.1. Critical Micelle Concentration Measurement

There are a number of techniques used for measuring the critical micelle concentration (CMC) of surfactants, viz: surface tension, conductivity, and calorimetry. In this study, the CMC of QS was measured using the conductivity method. The concentration of QS used in the study ranged from 100 ppm to 1000 ppm. A conductivity meter (WTW inoLab, Model no.: Cond 7110; Conductivity range: 20 - 199.99 mS/cm, with resolution: 0.1 mS/cm; temperature range: −25˚C - +125˚C, with resolution: 0.1˚C) was used for the study. Initially, the conductivity meter was calibrated using a solution of known concentration and after each measurement, the probe was washed with deionised water. The electrical conductivity (in μS/cm) of different concentrations of the surfactant solution was measured using the conductivity meter (see Figure 6 for the Conductivity meter used in the study). The measurements were made at atmospheric pressure (101,325 Pa) and room temperature (25˚C).

The concentration of surfactant was then plotted against conductivity as shown in Figure 7. The CMC of QS is identified on the graph as the point where the gradient changes *i.e.* the point of intersection (or inflexion point).

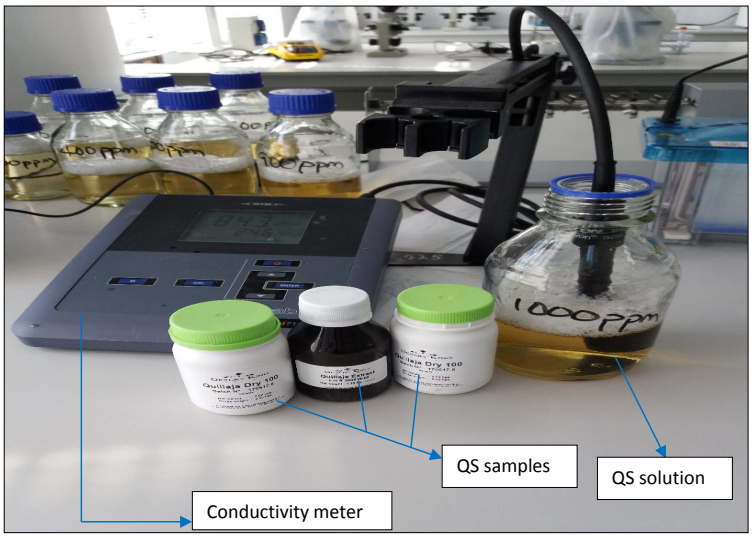

Figure 6. Conductivity meter used in the study.

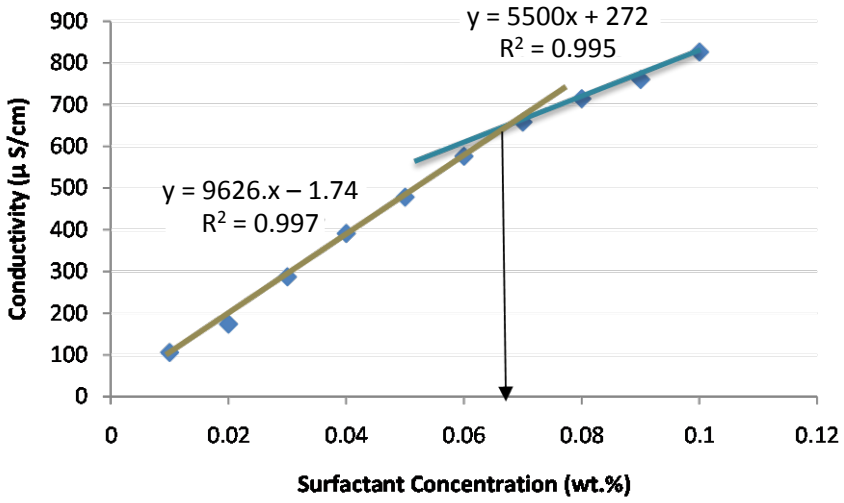

Figure 7. CMC of QS from conductivity measurements.

3.2. Adsorption Experiment

In this study, the batch equilibrium test was used to determine the adsorption of QS onto crushed sandstone rock samples. Over the duration of the test, weighed samples of the adsorbents were allowed to reach equilibrium with various initial concentrations of the surfactant ranging from 100 to 1000 ppm. Crushed sandstone samples and QS were mixed in the ratio of 1:8, *i.e.* 5 g of sandstone sample was mixed with 40 mL of QS in a test tube. The test tube was shaken vigorously to ensure uniform mixing. The concentration of the QS was measured before and after adsorption, and the difference between these concentrations gives the adsorption capacity q of the rock sample in mg/g, as presented in Equation (1).

$$q = \frac{m_{solution} \times \left(C^{o} - C\right)}{m_{sandstone}} \times 10^{-3} \tag{1}$$

In Equation (1), q is adsorption density onto rock surface (mg/g –rock), $m_{solution}$ is the total mass of solution in the original bulk solution (g), C^{o} is the initial surfactant concentration before adsorption (mg/L), C is the surfactant concentration after adsorption (mg/L), and $m_{sandstone}$ is total mass of crushed sandstone (g).

Regular concentration measurements of the mixture were taken over a period of time and equilibrium or steady state condition was reached after 108 hours in the initial test. Two more runs of the experiments were conducted and a good match was obtained with the preliminary test and with a percentage error of about 2%, the results for the last 2 runs were used for analysis. It is worthy of note that the conductivity method was used to determine the differences in concentration during the adsorption experiments. Figure 8 represents the adsorption of different concentrations of QS on sandstone.

Figure 9, on the other hand, represents the adsorbed amount of QS onto sandstone at different equilibrium concentrations of QS; as the equilibrium concentration of QS increases, so also does the adsorbed amount of QS on sandstone, though this increase slows down at higher equilibrium QS concentration.

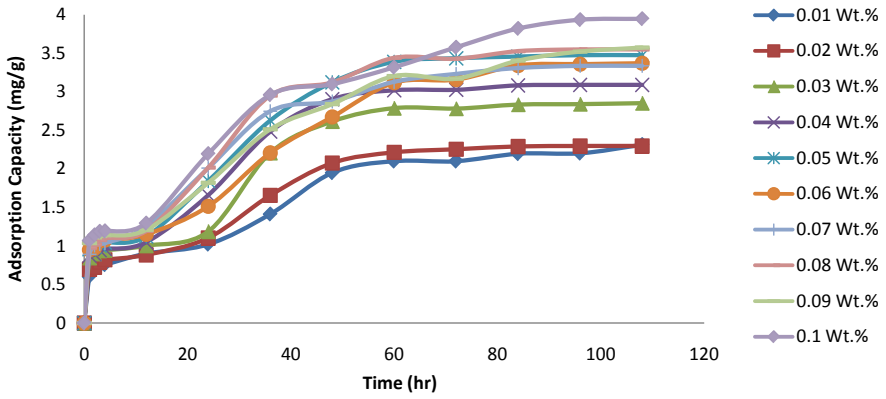

Figure 8. Adsorption capacity versus time for different surfactant concentrations.

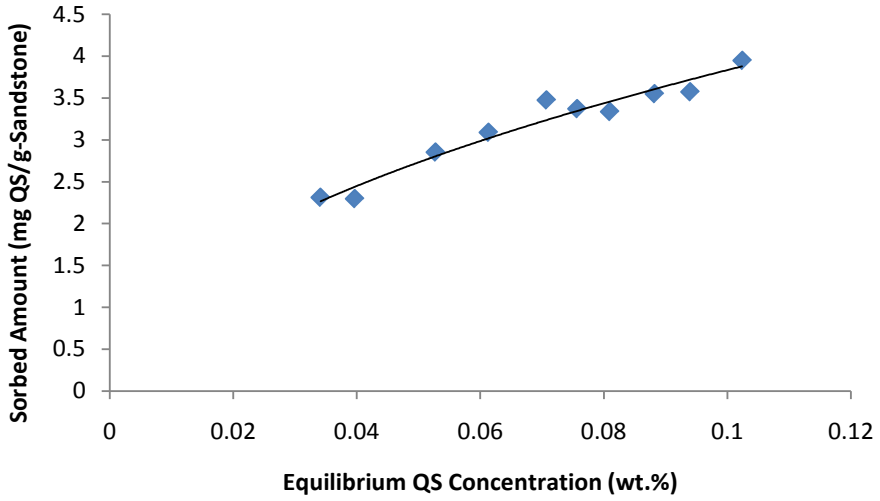

Figure 9. Equilibrium sorption isotherm for different QS concentrations.

3.3. Adsorption Isotherm Models

Adsorption is a process that involves solid-liquid interaction as well as mass transfer from the aqueous to the solid phase. An equilibrium adsorption isotherm model is a mathematical equation which shows the relationship between equilibrium surfactant adsorption at the solid-liquid interface and the equilibrium concentration of surfactant in solution [46]. In order words, an adsorption isotherm model is required to predict the amount of loading on the adsorption matrix at a given concentration of the adsorbate [23]. On the other hand, the adsorption kinetic models are used to predict the adsorption rate and thus provide information about the adsorption mechanism. Some notable adsorption isotherms models, available in literature, are presented herein.

3.3.1. Langmuir Isotherm

The Langmuir isotherm is one of the foremost adsorption models [47] [48] [49]. This model is based on 3 assumptions, viz: monolayer coverage, homogeneous adsorption sites, and identical sorption sites with equivalent energy. Based on these assumptions, the Langmuir isotherm equation is:

$$q_e = \frac{q_o K_L C_e}{1 + K_L C_e} \tag{2}$$

Langmuir isotherm parameters can be determined by the linearization of the isotherm equation:

$$\frac{1}{q_e} = \frac{1}{q_o} + \frac{1}{q_o K_L C_e} \tag{3}$$

where, q_e is amount of surfactant adsorbed per gram of adsorbent (crushed rock) at equilibrium (mg/g); q_o is maximum monolayer coverage capacity (mg/g); C_e is equilibrium concentration of adsorbate (mg/L); K_L is Langmuir isotherm constant (L/mg). The values of q_o and K_L are obtained from the intercept and slope respectively of the Langmiur plot of $1/q_e$ versus $1/C_e$. A key part of the Langmuir isotherm is the dimensionless quantity known as separation factor or equilibrium parameter [50]

$$R_L = \frac{1}{1 + K_L C_e} \tag{4}$$

The R_L value determines the nature of the adsorption process to be either unfavourable if $R_L > 1$, linear if $R_L = 1$, favourable if $0 < R_L < 1$, and irreversible if $R_L = 0$ [51]. The Langmuir isotherm constant K_L is a measure of the affinity between the adsorbent and the adsorbate molecules; higher magnitude of K_L implies stronger affinity of adsorbent for adsorbate molecules.

Figure 10 presents the QS adsorption kinetics result for the Langmuir isotherm at 298K, which shows that the relationship between $1/q_e$ and $1/C_e$ is linear, therefore an increase in $1/q_e$ results in a similar increase in $1/C_e$.

3.3.2. Freundlich Isotherm

The Freundlich isotherm is commonly used to describe the adsorption characteristics for heterogeneous surfaces, *i.e.* for non-ideal adsorption processes. This isotherm typically does not predict any saturation of the adsorbent by the adsorbate [52]; this implies that an infinite surface coverage is likely to occur, resulting in a multilayer coverage of the surface. The equation for this model is given as:

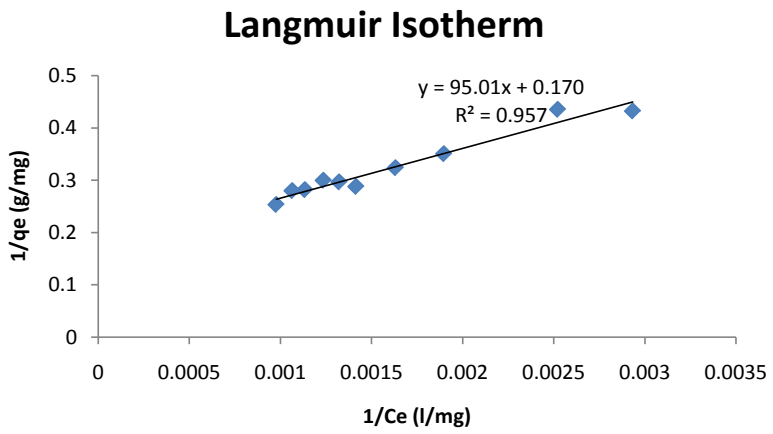

Figure 10. Langmuir isotherm for different QS concentrations at 298K.

$$q_e = K_F C_e^{1/n} \tag{5}$$

where: q_e is the amount of surfactant adsorbed per gram of the adsorbent (crushed rock) at equilibrium (mg/g); K_F is the Freundlich isotherm constant (mg/g); n is the adsorption intensity; and C_e is the equilibrium concentration of adsorbate (mg/L).

The linearised format is:

$$\log q_e = \log K_F + \frac{1}{n} \log C_e \tag{6}$$

Figure 11 is QS adsorption kinetics results from Freundlich isotherm at 298K. This shows that there is a linear relationship between the logarithm of the amount of QS per gram of sandstone (mg/g), and the logarithm of equilibrium concentration of adsorbate (mg/L).

3.3.3. Temkin Isotherm

The Temkin isotherm model contains a factor that takes into account the adsorbent-adsorbate interactions. Aharoni and Tompkins (1970) claimed that the adsorption heat of the molecules present in the adsorbed layer declines linearly with coverage due to the interactions [53]. The Temkin equation is represented as:

$$q_e = B \ln K_T + B \ln C_e \tag{7}$$

where: B is the constant related to heat of sorption (J/mol); K_T is Temkin isotherm equilibrium constant (L/g); q_e is the amount of surfactant adsorbed per gram of adsorbent (crushed rock) at equilibrium (mg/g); and C_e is the equilibrium concentration of adsorbate (mg/L). The constant B is further expressed as:

$$B = \frac{RT}{b_T} \tag{8}$$

where:

R = universal gas constant

T = operational temperature

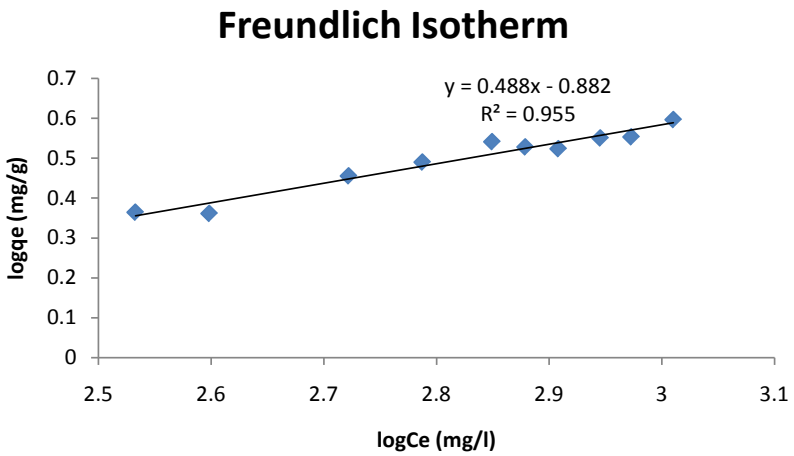

Figure 11. Freundlich isotherm for different QS concentrations at 298K.

b_T = Temkin Isotherm constant

Temkin isotherm results at 298K for QS are presented in Figure 12; this is a plot of q_e versus $\ln C_e$, where the amount of QS adsorbed per gram of sandstone (mg/g) increases with the natural logarithm of the equilibrium concentration of adsorbate (mg/L).

3.3.4. Henry's Law Model

The Henry's law model, also known as the linear isotherm model, is expressed as:

$$q_e = K_H C_e \tag{9}$$

where: q_e is the amount of surfactant adsorbed at equilibrium (mg/g); C_e is the equilibrium concentration of adsorbent (mg/L); and K_H is Henry's constant (L/m^2).

In Figure 13, Henry's law, or the linear isotherm model demonstrates that the equilibrium amount of QS adsorbed on sandstone (mg/g) is directly proportional to the equilibrium concentration of adsorbent (mg/L)

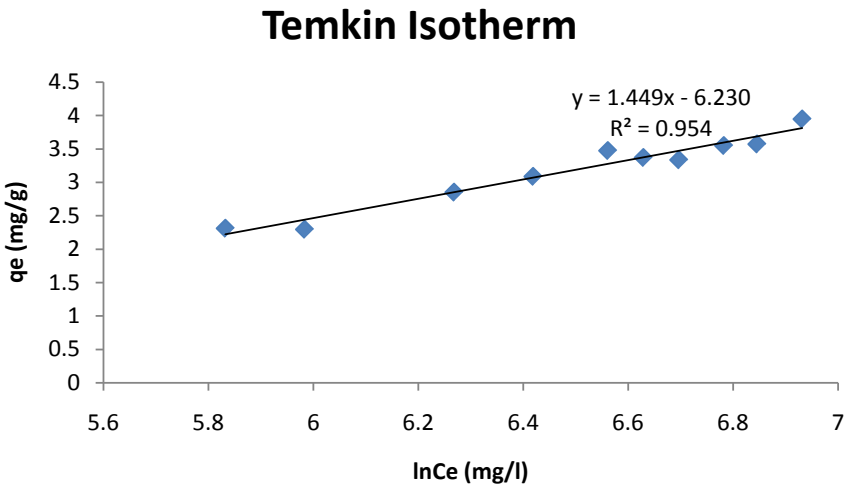

Figure 12. Temkin isotherm for different QS concentrations at 298K.

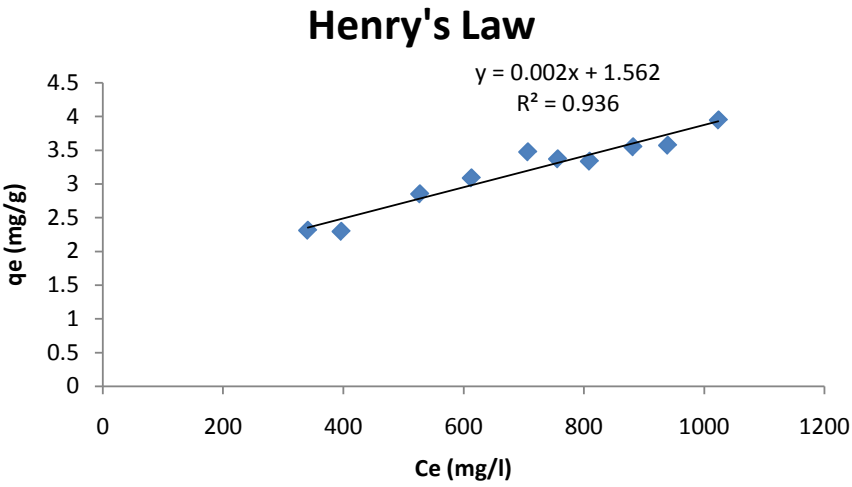

Figure 13. Linear isotherm for different QS concentrations at 298K.

3.4. Theory of Adsorption Kinetics

For the purpose of studying the adsorption kinetics of QS on sandstone crushed rock, three widely used models were employed, namely: pseudo-first-order, pseudo-second-order, and intra-diffusion models. The kinetic study was performed at 25˚C (room temperature); the amount of QS adsorbed by the sandstone was recorded over time and this is presented in **Figure 8**.

3.4.1. Pseudo-First-Order Kinetic Model

Lagergren (1898) proposed a method for studying adsorption kinetics known simply as the pseudo-first-order kinetic model [54]. The differential form of the equation is:

$$\frac{\mathrm{d}q_t}{\mathrm{d}t} = k_1\left(q_e - q_t\right) \tag{10}$$

where: q_e (mg/g) and q_t (mg/g) are the amounts of adsorbed adsorbate at equilibrium and at time t, respectively, and k_1 (hr^{-1}) is the rate constant of pseudo-first-order adsorption. By integrating Equation (9) over the boundary condition: $t = 0, q_t = 0$; $t = t, q_t = q_t$, the equation simplifies to:

$$\ln\left(q_e - q_t\right) = \ln q_e - k_1 t \tag{11}$$

3.4.2. Pseudo-Second-Order Kinetic Model

The differential form of the pseudo-second-order kinetic equation [55]:

$$\frac{\mathrm{d}q_t}{\mathrm{d}t} = k_2\left(q_e - q_t\right)^2 \tag{12}$$

By integrating Equation (10), the linear form of the equation is obtained as:

$$\frac{t}{q_t} = \frac{1}{k_2 q_e^2} + \frac{1}{q_e}t \tag{13}$$

where: k_2 is the equilibrium rate constant (g/mg-hr) of the pseudo-second-order model. The plot of t/q_t against t will give a linear relationship, from which k_2 and q_e can be determined from the slope and intercept of the graph. The pseudo-second-order kinetics equation is known to be able to predict the kinetic behaviour of a wide variety of adsorption systems, such as metal ions, herbicides, dyes, etc, over a range of process conditions [53]. Two parameters of importance in this kinetic model are initial adsorption rate, h, and half-adsorption time $t_{1/2}$, which are both expressed as:

$$h = k_2 q_e^2 \tag{14}$$

$$t_{1/2} = \frac{1}{k_2 q_e} \tag{15}$$

3.4.3. Intra-Particle Diffusion Model

Internal and external diffusion are essential parts of the adsorption processes. As a result, it was discovered that in most adsorption systems, the amount of solute q_t on the surface of the sorbent (mg/g) is a linear function of $t^{1/2}$ rather than the

contact time, t.

The intra-particle diffusion equation is given as [56]:

$$q_t = k_i t^{1/2} \tag{16}$$

where k_i is the intraparticle diffusion rate constant (mg/g $hr^{1/2}$).

4. Error Analysis

As a result of the bias inherent in the linearization of the 4 adsorption isotherm models, alternative isotherm parameters were determined using non-linear regression. This provides a mathematically rigorous method for determining adsorption isotherm parameters from the original form of the isotherm equation [57] [58]. In addition to the coefficient of determination or R^2 value, this study also employed the absolute relative deviation (ARD) or the normalised percent deviation (the P criterion) [59], as well as the chi-square test χ^2. These parameters are defined by the following equations:

$$\text{ARD} = \frac{100}{n}\sum_{i=1}^{n}\left|\frac{q_i^{exp} - q_i^{model}}{q_i^{exp}}\right| \tag{17}$$

$$\chi^2 = \sum_{i=1}^{n}\frac{\left(q_i^{exp} - q_i^{model}\right)^2}{q_i^{exp}} \tag{18}$$

where q^{exp} is the measured, experimental value of surfactant adsorption at any concentration C_e, q^{model} is the corresponding predicted surfactant adsorption according to the adsorption equation under study and n is the number of observations. Relatively smaller ARD and chi-square coupled with high coefficient of determination, R^2 values imply that the model is more able to predict experimental adsorption data with acceptable accuracy.

The quality, and thus reliability of experimental result is dependent on how closely it matches the adsorption model. The ARD and chi-square test results are presented in **Table 4**.

5. Results and Discussion

5.1. Critical Micelle Concentration (CMC) Determination

The CMC of QS was determined using the conductivity method as outlined in the experimental investigation section. At low QS concentration, the molecules arrange at the surface. As the surfactant concentration increased, the conductivity also increased. At a particular QS concentration, the molecules started to agglomerate and thus form aggregates or micelles, causing the electrical conductivity of the surfactant solution to experience a sudden change. This concentration at which the molecules of QS form micelles, known as the CMC, is depicted as an abrupt change in its electrical conductivity as shown in **Figure 7**. In this study, the CMC of QS is observed to be 0.068 wt% (for QS with 23.4% saponin content).

The CMC of saponins derived from QS have been reported extensively in lite-

rature. Mitra and Dungen (1997) reported relatively high CMC values, ranging from 0.051 to 0.072 wt% at 298K [60]. Mid and lower CMC values have also been presented, they include: 0.025 wt% by Stanimirova *et al.* (2011) [40], 0.010 to 0.020 wt% by Chen *et al.* (2008) for QS with 13.9% purity level [61], and 0.003 to 0.015 wt% reported by Zhou *et al.* (2011) for QS with 10% saponin content [62]. In this study using QS with 23.4% purity level, the CMC was determined to be 0.068 wt%, which is within the range of CMC values presented by other researchers herein. Researchers have attributed the differences in CMC value to different manufacturers who obtain their raw material from a wide variety of sources and plant parts, as well as to the differences in the extraction process.

While the CMC value is useful for describing the overall adsorption of QS onto sandstone, it is also important for determining the range of QS concentration that would be applicable for enhanced oil recovery studies.

5.2. Adsorption at Equilibrium Concentrations/Effect of Initial Surfactant Concentration

Figure 9 shows the amount of adsorbed surfactant in mg per unit g of sandstone over a range of equilibrium concentrations. It can be seen that the sorbed amount of QS increases sharply from low to high equilibrium concentration and reaches a peak at the CMC, *i.e.* an increase in the concentration of QS leads to a corresponding rise in adsorption capacity of sandstone. This can be attributed to the increasing difference between the exposed sandstone surface and the bulk QS solution. Another important take away from the figure is that at the critical micelle concentration (0.068 wt%), the adsorption capacity of QS is about 3.6 mg/g of sandstone. Beyond the CMC, the aqueous monomer concentration will not increase with any further addition of surfactant since the additional surfactant will only form more micelles [37].

5.3. Effect of Residence Time

An important aspect of this study is the effect of contact or residence time on the efficiency of surfactant adsorption on sandstone rock samples. This is particularly useful for understanding the kinetics of the adsorption process. As shown in **Figure 8**, the maximum amount of adsorption of QS occurs at about 108 hours. The graph indicates that as the initial concentration of QS increases, so does the adsorption rate. The increase is initially fast but slows down and subsequently reaches equilibrium after almost 5 days. This could be attributed to the fact that at the start of the adsorption reaction, the available surface area of the sandstone sample is high. As time progressed, a single layer is formed by the adsorbed surfactant, thereby causing a reduction in the adsorption capacity of the adsorbent. Subsequent adsorption is thus driven not by the concentration gradient but by the rate at which the surfactant can be transported from the exterior to the interior sites of the adsorbent. With time, the rate of adsorption decreases due to the very slow rate of diffusion of the solute particles into the bulk of the adsorbent, and ultimately reaches steady state, when no further adsorption takes

place, *i.e.* no change in adsorption tendency with respect to time.

5.4. Adsorption Isotherm Study

In this study, only the 2-parameter adsorption isotherm models, namely Langmuir, Fruendlich, Temkin, and Linear (Henry's Law), were studied at 298K. Adsorption isotherms are characterised by parameters that depict adsorbent surface properties as well as the affinity of the adsorbent for the adsorbate. Table 2 shows the correlations for each of the 4 adsorption isotherms used at 298K. In the case of the Langmuir isotherm, $1/q_e$ was plotted against $1/c_e$ in order to determine the equilibrium behaviour of the QS in the presence of crushed sandstone. This is shown graphically in Figure 10. The magnitude of the Langmuir constants, namely q_o, K_L, and R_L, are presented in Table 2. The value of $R_L = 0.353169$ indicates that the adsorption of QS on sandstone is a favourable adsorption process. However, a K_L value of about 0.001789 shows that the affinity of sandstone molecules for QS molecules is not strong [51]. This is of particular importance in chemical EOR as it implies that the loss (or adsorption) of QS in the surfactant flooding of a sandstone reservoir would be minimal, thereby keeping the cost of surfactants to an affordable value.

To understand the Freundlich isotherm, a graph of $\log q_e$ versus $\log c_e$ was plotted, and the constants $1/n$ and K_F were determined. The graph (Figure 11) shows a fairly good agreement between experimental and model data, with a correlation coefficient of 0.955. The comparatively slightly lower coefficient of determination may be due to the reasonably homogenous surface of the adsorbent (sandstone), which is not well suited to the Freundlich adsorption isotherm. The not-so-perfect fit of the Freundlich isotherm model is corroborated by both the P criterion and chi-square test values shown in Table 4, which are higher than those of the Langmuir isotherm. The adsorption parameters of the Temkin isotherm are obtained from a plot of q_e versus $\ln C_e$ (Figure 12). Table 2 presents

Table 2. Adsorption isotherm paramaters at 298K.

q_o (mg/g)	Langmuir Correlation: $1/q_e = 95.01/C_e + 0.170$		
	K_L (L/mg)	R_L	R^2
5.88235	0.001789	0.353169	0.958
$1/n$	Freudlich Correlation: $\log q_e = 0.488 \log C_e - 0.882$		
	n	K_F (mg/g)	R^2
0.488	2.049180	0.13121	0.956
B	Temkin Correlation: $q_e = 1.44 \ln C_e - 6.230$		
	b_T	K_T (L/mg)	R^2
1.44	1720.53611	0.0132	0.955
K_H (L/g)	Henry's Model Correlation: $q_e = 0.002C_e + 1.562$		
	Constant, C	-	R^2
0.002	1.562	-	0.936

the model parameters and, given the correlation of determination value, it is obvious that the Temkin adsorption model is not good enough to describe the equilibrium adsorption behaviour of QS on sandstone rock. Lastly, a plot of q_e against C_e (Figure 13), which describes the Henry's law or linear adsorption isotherm model, was used to obtain equilibrium adsorption parameters. The R^2 value obtained fell short of properly elucidating the adsorption characteristics of the surfactant at equilibrium conditions. Table 3 shows the experimental adsorption capacity of sandstone and compares it with the predicted values for all 4 adsorption isotherm models.

Using a combination of these correlations and regression analysis, the appropriate isotherm model can be obtained and used to optimally design an adsorption system for use in EOR. Based on the correlation coefficient or the R^2 value, the Langmuir isotherm with a value of 0.958 represents the adsorption experimental data most appropriately, compared to the Freundlich, Temkin, and Linear isotherms with R^2 values of 0.956, 0.955, and 0.936 respectively. However, only the R^2 value is not a sufficient criterion for data fitting. By combining the R^2, ARD and chi-square criteria (in Table 4), the best isotherm model can be found. It can be concluded that the Langmuir adsorption isotherm represents the experimental data of QS at 298K better than the other 3 models.

5.5. Adsorption Kinetics

In order to evaluate the adsorption results, 3 well known adsorption kinetic models

Table 3. Experimental and model predicted adsorption capacity of sandstone on QS.

QS Conc. (wt%)	Expt. Adsorption Capacity q_e^{exp}	Langmuir Isotherm q_e^{model}	*Freundlich Isotherm* q_e^{model}	*Temkin Isotherm* q_e^{model}	*Linear Isotherm* q_e^{model}
0.01	2.312291	2.228949	2.259278	2.166382	0.682060
0.02	2.229157	2.441553	2.432117	2.383906	0.793280
0.03	2.852190	2.855630	2.794648	2.793906	1.054580
0.04	3.088432	3.077120	3.007911	3.010908	1.226100
0.05	3.474486	3.285008	3.224323	3.215923	1.413700
0.06	3.370770	3.382914	3.331851	3.313543	1.512860
0.07	3.336198	3.479604	3.444610	3.410936	1.618720
0.08	3.549392	3.600291	3.591603	3.534244	1.763440
0.09	3.572440	3.688057	3.704286	3.625400	1.878680
0.10	3.946970	3.805103	3.863168	3.749326	2.047520

Table 4. Statistical criterion for adsorption isotherm models.

	Langmuir	Freundlich	Temkin	Lninear
ARD (P Criterion)	2.880020	3.144580	2.880480	57.104407
χ^2	0.038368	0.041656	0.039561	10.135245

were examined. In the first case, QS adsorption on sandstone rock was modelled using the pseudo-first order kinetic equation by plotting $\ln(q_e - q_t)$ versus t. The slope and intercept of the straight line graph made it possible to determine the rate constant, K_1, and equilibrium adsorption rate q_e, respectively. Figure 14 is the adsorption kinetic plot for the pseudo-first order model, while Table 5 displays the adsorption parameters for this model for different surfactant concentrations. The results indicate that the adsorption of QS follow the Lagergren model only at very high concentrations, with very low correlation parameters ($R^2 < 0.7$). Consequently, this kinetic model does not sufficiently fit experimental results and therefore lacks the ability to fully explain the adsorption of QS onto sandstone.

For this study of the adsorption of QS on sandstone, Figure 15 is a plot of t/q_t versus t, and it depicts the adsorption rate by virtue of the pseudo-second order model. The graph is a straight line, and the second order rate constant K_2 and

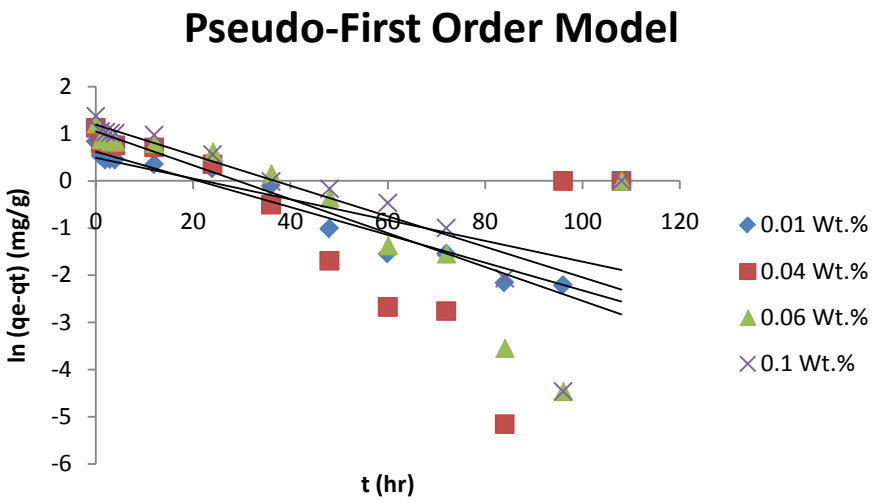

Figure 14. Adsorption kinetics for pseudo-first order model of QS on sandstone.

Table 5. Pseudo-First order adsorption kinetic model for QS.

Surfactant Conc. (wt%)	*Correlation*	K_1 (hr^{-1})	R^2
0.01	$\ln(q_e - q_t) = -0.022t + 0.488$	0.022	0.622
0.02	$\ln(q_e - q_t) = -0.026t + 0.325$	0.026	0.326
0.03	$\ln(q_e - q_t) = -0.038t + 0.736$	0.038	0.605
0.04	$\ln(q_e - q_t) = -0.029t + 0.620$	0.029	0.376
0.05	$\ln(q_e - q_t) = -0.028t + 0.791$	0.028	0.421
0.06	$\ln(q_e - q_t) = -0.035t + 1.048$	0.035	0.620
0.07	$\ln(q_e - q_t) = -0.024t + 0.724$	0.024	0.442
0.08	$\ln(q_e - q_t) = -0.025t + 0.785$	0.025	0.439
0.09	$\ln(q_e - q_t) = -0.026t + 0.998$	0.026	0.691
0.10	$\ln(q_e - q_t) = -0.032t + 1.189$	0.032	0.622

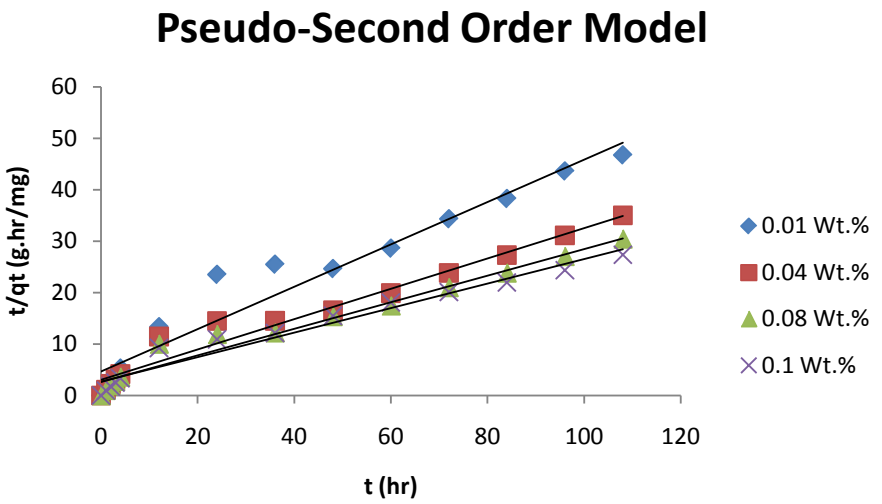

Figure 15. Adsorption kinetics for pseudo-second order adsorption model for QS on sandstone.

the equilibrium rate of adsorption q_e are obtained from the intercept and slope, respectively. In this model, the coefficient of determination (R^2) values are much higher, greater than 0.955 on the average, as shown in Table 6. Comparatively, the pseudo-second order kinetic model fits the experimental data more than its first-order counterpart. It is important to state that the fit of experimental and model adsorption capacity is much closer for all surfactant concentrations, especially around the critical micelle concentration of QS. The results for the pseudo-second order isotherm model also indicate that the adsorption rate constant is initially high, which implies therefore that the initial adsorption rate h is also low; the half-adsorption time, on the other hand, is low for QS on sandstone rock samples.

The kinetic behaviour of QS on sandstone was also investigated in relation to the intra-particle diffusion model. In order to use this model, q_t was plotted against $t^{1/2}$ and this should give a straight line graph. For adsorption systems where intra-particle diffusion is the controlling mechanism, this plot should be a straight line passing through the origin, which implies that the adsorption rate at any given time should be linearly (directly) proportional to the square root of the time. Based on the results presented in Figure 16 and Table 7, there are clearly other competing adsorption mechanisms other than intra-particle diffusion mechanism involved in the adsorption of QS on sandstone: the straight line graph does not pass through the origin for some surfactant concentrations and the R^2 value range between 0.925 and 0.969. This can be explained thus: during the first stage of adsorption, diffusion of the surfactant molecules occurs at the external surface of the sandstone, and this process was fast, occurring over the first 4 hours, and is depicted by a sharp slope in Figure 8. This is known as the boundary layer diffusion process [63]. In the second stage of adsorption, which occurs from hours 4 to about 24, the rate of diffusion of the QS molecules is controlled by the thickness of the boundary layer. This is known as the intra-particle diffusion

Table 6. Adsorption kinetic parameters for pseudo-second order model for different surfactant concentrations.

Surfactant Conc. (wt%)	*Correlation*	K_2 (g/mg.hr)	R^2
0.01	$t/q_t = 0.411t + 4.672$	0.036	0.947
0.02	$t/q_t = 0.401t + 4.062$	0.040	0.958
0.03	$t/q_t = 0.319t + 3.628$	0.028	0.937
0.04	$t/q_t = 0.295t + 3.012$	0.029	0.965
0.05	$t/q_t = 0.261t + 2.908$	0.023	0.959
0.06	$t/q_t = 0.273t + 3.405$	0.022	0.942
0.07	$t/q_t = 0.278t + 2.574$	0.030	0.978
0.08	$t/q_t = 0.258t + 2.592$	0.026	0.969
0.09	$t/q_t = 0.265t + 2.928$	0.024	0.960
0.10	$t/q_t = 0.238t + 2.650$	0.021	0.964

Table 7. Adsorption kinetic parameters for intra-particle diffusion model.

Surfactant Conc. (wt%)	Correlation	K_i (g/mg.hr)	R^2
0.01	$q_t = 0.207t^{0.5} + 0.279$	0.207	0.952
0.02	$q_t = 0.214t^{0.5} + 0.317$	0.214	0.941
0.03	$q_t = 0.271t^{0.5} + 0.351$	0.271	0.925
0.04	$q_t = 0.301t^{0.5} + 0.363$	0.301	0.939
0.05	$q_t = 0.340t^{0.5} + 0.364$	0.340	0.948
0.06	$q_t = 0.314t^{0.5} + 0.357$	0.314	0.958
0.07	$q_t = 0.318t^{0.5} + 0.425$	0.318	0.955
0.08	$q_t = 0.343t^{0.5} + 0.420$	0.343	0.946
0.09	$q_t = 0.322t^{0.5} + 0.439$	0.322	0.963
0.10	$q_t = 0.363t^{0.5} + 0.442$	0.363	0.969

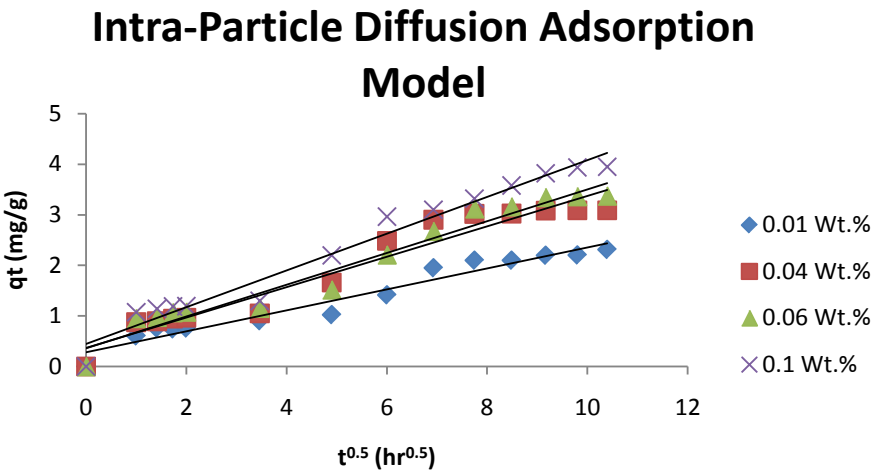

Figure 16. Adsorption kinetics for intra-particle diffusion model.

adsorption [63]. Therefore, the rate limiting step is a combination of both the boundary layer and intra-particle diffusion steps.

5.6. Quillaja Saponaria versus Synthetic Surfactants

The selection process for potential surfactants in chemical EOR is a very rigorous one. These surfactants go through a wide array of scrutiny before being considered suitable for pilot or field-scale usage. One of such is the technical feasibility of the surfactant, which entails adsorption and kinetics study. Additionally, a cost-benefit-analysis is also carried out, which takes into account the prevailing crude oil price and selling price of the surfactant in relation to how much oil recovery the surfactant is likely to bring about. It is important to point out that some of the common synthetic surfactants used in chemical EOR such as SDS, Tween-80, and Triton X-100 [36] [37] are synthesized via the ethoxylation reaction. This manufacturing process, which reacts ethylene oxide (EO) with phenols and alcohols, has been known to cause accidents due to the highly reactive and thermally-unstable nature of EO as reported by Trevor Kletz (1988) [64]. The process has also been attributed to the potential formation of 1,4-Dioxane, a known carcinogen [65]. Natural saponins such as QS, on the other hand, have been extracted by safe, cheap, simple-to-implement laboratory methods such as Soxhlet extraction followed by drying [22] [23] [39], which poses no health risk to users. This in turn significantly reduces the cost of employing natural surfactants such as QS in chemical EOR operations.

6. Future Work

The work undertaken in this research has shed more light into the adsorption properties of QS, particularly with regards to being used as a surfactant in chemical enhanced oil recovery. However, more work still remains to be done, especially in the following areas:

1) Effect of temperature changes on adsorption properties of QS.

2) Impact of using QS for increasing the recovery factor of oil reservoirs.

3) Use of QS to alter wettability of reservoir rocks from oil- to water-wet, thus making more oil available for recovery.

7. Conclusions

In this work, equilibrium and kinetic parameters for the adsorption of Quillaja Saponaria (QS) onto sandstone rock samples were studied with a view to obtaining results that could make QS a suitable surfactant candidate for chemical EOR. Adsorption parameters for 4 isotherm models, viz: Langmuir, Freundlich, Temkin and Linear, were also investigated. Additionally, the kinetic parameters for 3 notable models, namely Pseudo-First order, Pseudo-Second order, and Intra-particle diffusion, were studied and used to evaluate the performance of the novel surfactant. Some relevant conclusions from this study include:

1) QS saponins behave as non-ionic surfactants, with a critical micelle con-

centration of 0.068 wt%, an adsorption capacity of about 3 mg/g of sandstone at the CMC. A fairly low CMC value indicates that a lesser amount of QS is required in order to become useful for its intended purpose, which naturally leads to cost-savings.

2) As the concentration of QS increases, so does the adsorption capacity; while the slope for the initial surfactant concentration is high, that for higher concentration is comparatively low.

3) With an R^2 value of 0.958, with P criterion and Chi-square values of 2.88 and 0.038, respectively, the Langmuir adsorption isotherm is the most appropriate model for describing the equilibrium adsorption behaviour of QS on sandstone rock.

4) The adsorption kinetics of QS is better suited to pseudo-second order model because the average R^2 value was 0.958 compared to 0.516 and 0.950 for first-order and intra-particle diffusion models, respectively.

Acknowledgements

The author is grateful to Messrs Pablo Jara and Matthieu Privat of Desert King S.A, Chile for providing the saponin samples and for numerous useful discussions. Gratitude also goes to Dr. Irada Khalilova of Khazar University for the use of the Biological Sciences laboratory.

Conflicts of Interest

The author declares no conflicts of interest regarding the publication of this paper.

References

[1] Ehrenberg, S.N. and Nadeau, P.H. (2005) Sandstone and Carbonate Petroleum Reservoirs: A Global Perspective on Porosity-Depth and Porosity-Permeability Relationships. *AAPG Bulletin*, **89**, 435-445. https://doi.org/10.1306/11230404071

[2] Bjørlykke, K. and Jahren, J. (2010) Sandstones and Sandstone Reservoirs. In: *Petroleum Geoscience*, Springer, Berlin, 113-140. https://doi.org/10.1007/978-3-642-02332-3_4

[3] Sheng, J.J. (2013) Surfactant Enhanced Oil Recovery in Carbonate Reservoirs. In: *Enhanced Oil Recovery*: *Field Case Studies*, Gulf Professional Publishing, Houston, 281-299. https://doi.org/10.1016/B978-0-12-386545-8.00012-9

[4] Enhanced Oil Recovery (EOR) (2006) Chemicals and Formulations. Akzo Nobel Surface Chemistry, Chicago, IL, 1-6.

[5] Marliere, C., Wartenberg, N., Fleury, M., Tabary, R., Dalmazzone, C. and Delamaide, E. (2015) Oil Recovery in Low Permeability Sandstone Reservoirs Using Surfactant-Polymer Flooding. *SPE Latin American and Caribbean Petroleum Engineering Conference*, Quito, 18-20 November 2015, Paper No. SPE-177072-MS. https://doi.org/10.2118/177072-MS

[6] Dong, Z., Zheng, Y. and Zhao, J. (2014) Synthesis, Physico-Chemical Properties and Enhanced Oil Recovery Flooding Evaluation of Novel Zwitterionic Gemini Surfactants. *Journal of Surfactants and Detergents*, **17**, 1213-1222. https://doi.org/10.1007/s11743-014-1616-z

[7] Liu, Y., Lu, Y., Lin, W. and Hu, X. (2011) Performance Study of a New Type Alkaline/Surfactant/Polymer Ternary Complex. *SPE Enhanced Oil Recovery Conference*, Kuala Lumpur, 19-21 July 2011, Paper No. SPE-145001-MS. https://doi.org/10.2118/145001-MS

[8] Zhang, X.-M., Guo, Y.-J., Liu, J.-X., Zhu, Y.-W., Hu, J., Feng, R.-S. and Fu, C.-Y. (2014) Adaptability of a Hydrophobically Associating Polyacrylamide/Mixed-Surfactant Combination Flooding System to the Shengli Chengdao Oilfield. *Journal of Applied Polymer Science*, **131**, Article ID: 40390. https://doi.org/10.1002/app.40390

[9] Hu, X.D., Tang, S.F., Liu, Y., Wen, S.C. and Yan, S.X. (2012) Performance of Anionic Gemini Surfactant in Enhancement of Oil Recovery. *Oilfield Chemistry*, **29**, 57-59, 79. (In Chinese) https://caod.oriprobe.com/articles/31767984/Performance_of_Anionic_Gemini_Surfactant_in_Enhancement_of_Oil_Recover.htm

[10] Bou-Mikael, S., Asmadi, F., Marwoto, D. and Cease, C. (2000) Minas Surfactant Field Trial Tests Two Newly Designed Surfactants with High EOR Potential. *SPE Asia Pacific Oil and Gas Conference*, Brisbane, 16-18 October 2000, Paper No. SPE-64288-MS. https://doi.org/10.2118/64288-MS

[11] Yin, D. and Pu, H. (2008) A Numerical Simulation Study on Surfactant Flooding and its Field Application in Daqing Oilfield. *SPE Europe/EAGE Annual Conference and Exhibition*, Rome, 9-12 June 2008, Paper No. SPE-112424-MS. https://doi.org/10.2118/112424-MS

[12] Liu, R.Q. (2013) Development of Enhanced Oil Recovery in Daqing. *Journal of Petroleum and Gas Engineering*, **4**, 46-50.

[13] Wang, H. and Miller, B. (2013) Development of a New Surfactant-Polymer System and Its Implementation in Daqing Oilfield. *Journal of Petroleum and Gas Engineering*, **4**, 118-126.

[14] Shah, D.O. and Schechter, R.S. (1977) Improved Oil Recovery by Surfactant and Polymer Flooding. Academic Press, Cambridge, 2.

[15] Hirasaki, G.J., Miller, C.A., Pope, G.A. and Jackson, R.E. (2004) Surfactant Based Enhanced Oil Recovery and Foam Mobility Control. 1st Annual Technical Report. DE-FC26-03NT15406. Rice University, Houston.

[16] Portwood, J.T. (2005) The Kansas Arbuckle Formation: Performance Evaluation and Lessons Learned from More than 200 Polymer-Gel Water-Shutoff Treatments. *SPE Production Operations Symposium*, Oklahoma City, 16-19 April 2005, Paper No. SPE-94096-MS. https://doi.org/10.2118/94096-MS

[17] Muthusamy, K., Gopalakrishnan, S., Ravi, T.K. and Sivachidambaram, P. (2008) Biosurfactants: Properties, Commercial Production and Application. *Current Science*, **94**, 736-747.

[18] Sobrinho, H.B.S., Luna, J.M., Rufino, R.D., Porto, A.L.F. and Sarubbo, L.A. (2014) Biosurfactants: Classification, Properties, and Environmental Applications. *Recent Developments in Biotechnology*, **11**, 1-29.

[19] Van Hamme, J.D., Singh, A. and Ward, O.P. (2006) Physiological Aspects: Part 1 in a Series of Papers Devoted to Surfactants in Microbiology and Biotechnology. *Biotechnology Advances*, **24**, 604-620. https://doi.org/10.1016/j.biotechadv.2006.08.001

[20] Bustamante, M., Durán, N. and Diez, M.C. (2012) Biosurfactants Are Useful Tools for the Bioremediation of Contaminated Soil: A Review. *Journal of Soil Science and Plant Nutrition*, **12**, 667-687. https://doi.org/10.4067/S0718-95162012005000024

[21] Bengtsson, T. (2013) Boosting Potato Defence against Late Blight—A Study from Field to Molecule. Ph.D. Thesis, Swedish University of Agricultural Sciences, Alnarp.

[22] Zendehboudi, S., Ahmadi, M.A., Rajabzadeh, A.R., Mahinpey, N. and Chatzis, I. (2013) Experimental Study on Adsorption of a New Surfactant onto Carbonate Reservoir Samples—Application to EOR. *Canadian Journal of Chemical Engineering*, **91**, 1439-1449. https://doi.org/10.1002/cjce.21806

[23] Ahmadi, M.A. and Shadizadeh, S.R. (2012) Adsorption of Novel Nonionic Surfactant and Particles Mixture in Carbonates: Enhanced Oil Recovery Implication. *Energy Fuel*, **26**, 4655-4663. https://doi.org/10.1021/ef300154h

[24] Zhang, R. and Somasundaran, P. (2006) Advances in Adsorption of Surfactants and Their Mixtures at Solid-Solution Interfaces. *Advances in Colloid Interface Science*, **123**-**126**, 216-229. https://doi.org/10.1016/j.cis.2006.07.004

[25] Paria, S. and Khilar, K.C. (2004) A Review on Experimental Studies of Surfactant Adsorption at the Hydrophilic Solid-Water Interface. *Advances in Colloid and Interface Science*, **110**, 75-95. https://doi.org/10.1016/j.cis.2004.03.001

[26] Somasundaran, P. and Huang, L. (2000) Adsorption/Aggregation of Surfactants and their Mixtures at Solid-Liquid Interfaces. *Advances in Colloid and Interface Science*, **88**, 179-208. https://doi.org/10.1016/S0001-8686(00)00044-0

[27] Dick, S.G., Fuerstenau, D.W. and Healy, T.W. (1971) Adsorption of Alkylbenzene Sulfonate (A.B.S.) Surfactants at the Alumina-Water Interface. *Journal of Colloid and Interface Science*, **37**, 595-602. https://doi.org/10.1016/0021-9797(71)90337-7

[28] Fuerstenau, D.W. and Wakamatsu, T. (1975) Effect of pH on the Adsorption of Sodium Dodecane-Sulfonate at the Alumina/Water Interface. *Faraday Discussions of the Chemical Society*, **59**, 157-168. https://doi.org/10.1039/dc9755900157

[29] Wu, S.H. and Pendleton, P. (2001) Adsorption of Anionic Surfactant by Activated Carbon: Effect of Surface Chemistry, Ionic Strength, and Hydrophobicity. *Journal of Colloid and Interface Science*, **243**, 306-315. https://doi.org/10.1006/jcis.2001.7905

[30] Ball, B. and Fuerstenau, D.W. (1971) Thermodynamics and Adsorption Behaviour in the Quartz/Aqueous Surfactant System. *Discussions of the Faraday Society*, **52,** 361-371. https://doi.org/10.1039/df9715200361

[31] Bavière, M., Ruaux, E. and Defives, D. (1993) Sulfonate Retention by Kaolinite at High pH—Effect of Inorganic Anions. *SPE Reservoir Engineering*, **8**, 123-127. https://doi.org/10.2118/21031-PA

[32] Curbelo, F.D.S., Santanna, V.C., E.L.B., Neto, E.L.B., Dutra Jr., T.V, Dantas, T.N.C., Neto, A.A.D. and Garnica, A.I.C. (2007) Adsorption of Nonionic Surfactants in Sandstone. *Colloids and Surfaces A*: *Physicochemical and Engineering Aspects*, **293**, 1-4. https://doi.org/10.1016/j.colsurfa.2006.06.038

[33] Bera, A., Kumar, T., Ojha, K. and Mandal, A. (2013) Adsorption of Surfactants on Sand Surface in Enhanced Oil Recovery: Isotherms, Kinetics and Thermodynamic Studies. *Applied Surface Science*, **284**, 87-99. https://doi.org/10.1016/j.apsusc.2013.07.029

[34] Beach, Brian A. (2016) Evaluation of an Alternative Natural Surfactant for Non Aqueous Phase Liquid Remediation. MSc. Thesis, Western Michigan University, Kalamazoo. http://scholarworks.wmich.edu/masters_theses/680

[35] Holmberg, K., Jönsson, B., Kronberg, B. and Lindman, B. (2003) Adsorption of Surfactants at Solid Surfaces. In: Holmberg, K., Jönsson, B., Kronberg, B. and Lindman, B., Eds., *Surfactants and Polymers in Aqueous Solution*, 2nd Edition, John Wiley & Sons, Hoboken, 357-387.

[36] Scamehorn, J.F. (1980) Equilibrium Adsorption of Surfactants on Mineral Oxide Surfaces from Aqueous Solutions. University of Texas at Austin, Austin.

[37] Muherei, M.A. and Junin, R. (2009) Equilibrium Adsorption Isotherms of Anionic, Nonionic Surfactants, and Their Mixtures to Shale and Sandstone. *Modern Applied Science*, **3**, 158-167. https://doi.org/10.5539/mas.v3n2p158

[38] Azam, M.R., Tan, I, M., Ismail, L., Mushtaq, M., Nadeem, M. and Sagir, M. (2013) Static Adsorption of Anionic Surfactant onto Crushed Berea Sandstone. *Journal of Petroleum Exploration and Production Technology*, **3**, 195-201. https://doi.org/10.1007/s13202-013-0057-y

[39] Ahmadi, M.A. and Shadizadeh, S.R. (2016) Adsorption of a Nonionic Surfactant onto a Silica Surface. *Energy Sources*, *Part A*: *Recovery*, *Utilization*, *and Environmental Effects*, **38**, 1455-1460. https://doi.org/10.1080/15567036.2011.652761

[40] Stanimirova, R., Marinova, K., Tcholakova, S., Denkov, N.D., Stoyanov, S. and Pelan, E. (2011) Surface Rheology of Saponin Adsorption Layers. *Langmuir*, **27**, 12486-12498. https://doi.org/10.1021/la202860u

[41] van Setten, D.C. and van de Werken, G. (1996) Molecular Structures of Saponins from *Quillaja saponaria* Molina. In: Waller, G.R. and Yamasaki, K., Eds., *Saponins Used in Traditional and Modern Medicine*. *Advances in Experimental Medicine and Biology*, Vol. 404, Springer, Boston, 185-193. https://doi.org/10.1007/978-1-4899-1367-8_17

[42] Suarez, T.S. (2015) Seasonal Analysis of Saponin Content of Leaves of Young Quillaja Saponaria Tress from a Plantation. MSc. Thesis, Pontifica Universidad Catolica de Chile, Santiago de Chile.

[43] Arif, T, Bhosale, J.D., Kumar, N., Mandal, T.K., Bendre, R.S., Lavekar, G.S. and Dabur, R. (2009) Natural Products-Antifungal Agents Derived from Plants. *Journal of Asian Natural Products Research*, **11**, 621-638. https://doi.org/10.1080/10286020902942350

[44] Moghimipour, E. and Handali, S. (2015) Saponin: Properties, Methods of Evaluation and Applications. *Annual Research and Review in Biology*, **5**, 207-220. https://doi.org/10.9734/ARRB/2015/11674

[45] Siram, K., Raghavan, C.V., Marslin, G., Rahman, H., Selvaraj, D., Balajumar, K. and Franklin, G. (2016) Quillaja Saponin: A Prospective Emulsifier for the Preparation of Solid Lipid Nanoparticles. *Colloids and Surfaces B*: *Biointerfaces*, **147**, 274-280. https://doi.org/10.1016/j.colsurfb.2016.07.065

[46] Barati-Harooni, A., Najafi-Marghmaleki, A., Tatar, A. and Mohammadi, A.H. (2016) Experimental and Modelling Studies on Adsorption of a Nonionic Surfactant on Sandstone Minerals in Enhanced Oil Recovery Process with Surfactant Flooding. *Journal of Molecular Liquids*, **220**, 1022-1032. https://doi.org/10.1016/j.molliq.2016.04.090

[47] Langmuir, I. (1916) The Constitution and Fundamental Properties of Solids and Liquids: Part 1: Solids. *Journal of American Chemical Society*, **38**, 2221-2295. https://doi.org/10.1021/ja02268a002

[48] Langmuir, I. (1918) The Adsorption of Gases on Plane Surfaces of Glass, Mica and Platinum. *Journal of American Chemical Society*, **40**, 1361-1403. https://doi.org/10.1021/ja02242a004

[49] Langmuir, I. (1917) The Constitution and Fundamental Properties of Solids and Liquids: Part II: Liquids. *Journal of American Chemical Society*, **39**, 1848-1906. https://doi.org/10.1021/ja02254a006

[50] Webber, T.N. and Chakravarti, R.K. (1974) Pore and Solid Diffusion Models for Fixed-Bed Adsorbers. *AIChE Journal*, **20**, 228-238. https://doi.org/10.1002/aic.690200204

[51] Ayad, M.M. and El-Nasr, A.A. (2010) Adsorption of Cationic Dye (Methylene Blue) from Water Using Polyaniline Nanotubes Base. *Journal of Physical Chemistry C*, **114**, 14377-14383. https://doi.org/10.1021/jp103780w

[52] Freundlich, H. (1906) Über die Adsorption in Lösungen. *Zeitschrift für Physikalische Chemie*, **57**, 385-470. https://doi.org/10.1515/zpch-1907-5723

[53] Aharoni, C. and Tompkins, F.C. (1970) Kinetics of Adsorption and Desorption and the Elovich Equation. In: Eley, D.D., Pines, H. and Weisz, P.B., Eds., *Advances in Catalysis*, Vol. 21, Academic Press, New York, 1-49. https://doi.org/10.1016/S0360-0564(08)60563-5

[54] Lagergren, S. (1898) About Theory of So-Called Adsorption of Soluble Substances. *Kungliga Svenska Vetenskapsakademiens Handlingar*, **24**, 1-39.

[55] Bulut, E., Özacar, M. and Şengil, İ.A. (2008) Adsorption of Malachite Green onto Bentonite: Equilibrium and Kinetic Study and Process Design. *Microporous and Mesoporous Materials*, **115**, 234-246. https://doi.org/10.1016/j.micromeso.2008.01.039

[56] Cheung, W.H., Szeto, Y.S. and McKay, G. (2007) Intraparticle Diffusion Processes during Acid Dye Adsorption onto Chitosan. *Bioresource Technology*, **98**, 2897-2904. https://doi.org/10.1016/j.biortech.2006.09.045

[57] Ho, Y.-S. (2004) Selection of Optimum Sorption Isotherm. *Carbon*, **42**, 2115-2116. https://doi.org/10.1016/j.carbon.2004.03.019

[58] Seidel, A. and Gelbin, D. (1988) On Applying the Ideal Adsorbed Solution Theory to Multicomponent Adsorption Equilibria of Dissolved Organic Components on Activated Carbon. *Chemical Engineering Science*, **43**, 79-89. https://doi.org/10.1016/0009-2509(88)87128-8

[59] Ayranci, E. and Duman, O. (2007) Removal of Anionic Surfactants from Aqueous Solutions by Adsorption onto High Area Activated Carbon Cloth Studied by *in Situ* UV Spectroscopy. *Journal of Hazardous Materials*, **148**, 75-82. https://doi.org/10.1016/j.jhazmat.2007.02.006

[60] Mitra, S. and Dungan, S.R. (1997) Micellar Properties of Quillaja Saponins. 1. Effects of Temperature, Salt and pH on Solution Properties. *Journal of Agricultural and Food Chemistry*, **45**, 1587-1595. https://doi.org/10.1021/jf960349z

[61] Chen, W.-J., Hsaio, L.-C. and Chen, K.K.-Y. (2008) Metal Desorption from Copper(II)/Nickel(II)-Spiked Kaolin as a Soil Component Using Plant-Derived Saponin Surfactant. *Process Biochemistry*, **43**, 488-498. https://doi.org/10.1016/j.procbio.2007.11.017

[62] Zhou, W., Yang, J., Lou, L. and Zhu, L. (2011) Solubilization Properties of Polycyclic Aromatic Hydrocarbons by Saponin, a Plant-Derived Biosurfactant. *Environmental Pollution*, **159**, 1198-1204. https://doi.org/10.1016/j.envpol.2011.02.001

[63] Senthil Kumar, P., Ramalingam, S., Abhinaya, R.V., Dinesh Kirupha, S., Vidhyadevi, T. and Sivanesan, S. (2012) Adsorption Equilibrium, Thermodynamics, Kinetics, Mechanism and Process Design of Zinc(II) Ions onto Cashew Nut Shell. *Canadian Journal of Chemical Engineering*, **90**, 973-982. https://doi.org/10.1002/cjce.20588

[64] Kletz, T.A. (1988) Fires and Explosion of Hydrocarbon Oxidation Plants. *Plant/Operations Progress*, **7**, 226-230. https://doi.org/10.1002/prsb.720070406

[65] Gustin, J.-L. (2000) Safety of Ethoxylation Reactions. IChemE Symposium Series No. 147. IChemE, Rugby, UK.